Application of Optimal Control Theory to the Design of the NASA/JPL 70-Meter Antenna Axis Servos

L. S. Alvarez and J. Nickerson
Ground Antenna and Facilities Engineering Section

The application of Linear Quadratic Gaussian (LQG) techniques to the design of the 70-m axis servos is described. Linear quadratic optimal control and Kalman filter theory are reviewed, and model development and verification are discussed. Families of optimal controller and Kalman filter gain vectors were generated by varying weight parameters. Performance specifications were used to select final gain vectors.

I. Introduction

This article presents the design of the position control algorithm for NASA's Deep Space Network antennas. The antennas are of an elevation over azimuth design and have two sets of transducers for measuring axis position. A 20-bit encoder is geared to the bull gear of each axis and measures angular displacements to approximately a third of a millidegree. Another position-sensing device is an autocollimator. The autocollimator measures the misalignment between an intermediate reference structure beneath the main paraboloid and a small reference antenna that is structurally isolated from the 70-m antenna. A control algorithm must be designed for both encoder feedback (known as the computer-mode control algorithm) and autocollimator feedback (known as the precision-mode control algorithm).

A state feedback controller with a constant gain estimator is used to close both the computer- and precision-mode control loops. The controller is based on a fifth-order state model with an added sixth state which integrates position error. A Kalman filter estimates state variables by using encoder feedback during both the computer and precision modes of opera-

tion. In the computer-mode algorithm, gains are applied to the integral error and position error (both formed from the position estimate and commanded position) and also applied to the remaining estimated states. In the precision-mode algorithm, control gains are similarly applied with the exception that now the estimated position error is replaced by the hardware-filtered autocollimator error and the integral error is numerically calculated based on this same error signal. The present implementation of the algorithm allows for different gains to be used for the computer and precision modes.

The objective is to design control and filter gains that minimize control effort while meeting performance characteristics, thereby reducing control system excitation of the lightly damped structure. This provides motivation to apply optimal control design techniques to determine controller gains.

Presented in this article are a brief review of optimal control theory and the step-by-step design process. The design process includes system model generation and the calculation of optimal controller and Kalman filter gains. The design methodology utilizes the Loop Transfer Recovery (LTR) method to calcu-

late the filter gains, and then both these and the state feedback gains are combined to form a Linear Quadratic Gaussian (LQG) controller. Most of the design procedure follows that reported in [1], but the estimator design is novel. Test results based on linear and nonlinear simulations are presented.

II. Theory

The LQG design method is applied to arrive at optimal linear output feedback control systems for the 70-m axis servos. The solution of the LQG problem is a combination of the Linear Quadratic Regulator (LQR) and Kalman filter problems. Both the optimal properties of LQG designs and the systematic nature of the design process served as motivation for its application. The design is separated into two problems: (1) designing a target closed-loop feedback control system using optimal control theory (specifically, an LQR control design is developed and then adapted for tracking), and (2) designing a Kalman filter to estimate inaccessible states.

A. The LQR Optimal Control Technique

The plant can be linearly modeled by a set of first-order differential equations of the form

$$\dot{x}(t) = Ax(t) + Bu(t) \quad ; \quad x(0) = x_0$$
$$y(t) = Cx(t) \tag{1}$$

where x is an n X 1 state column vector; u is an m X 1 input column vector; y is an m X 1 output column vector; and A, B, and C are coefficient matrices of appropriate dimensions. The control for a state variable feedback controller takes the form

$$u(t) = -Kx(t) \tag{2}$$

where K is a feedback gain vector, not necessarily producing an optimum controller. Substituting Eq. (2) into Eq. (1) yields

$$\dot{x}(t) = Ax(t) - BKx(t) = (A - BK)x(t) \tag{3}$$

The plant dynamics are thus modified by the feedback gain vector K.

State feedback is attractive because the closed-loop eigenvalues of the system are arbitrarily specified by the proper selection of the feedback vector K. Numerical procedures exist that calculate K for a desired set of eigenvalues [2]. Although a designer can iterate a pole selection until the closed-loop system meets performance criteria, there are no guarantees that the design is optimal.

The LQR optimal control problem to be presented is a specific example of a deterministic dynamic optimization problem. For a linear system, a quadratic performance index is used as a performance criterion. Given the system description in Eq. (1), the quadratic performance index J is of the form:

$$J = \int_0^\infty [x^T(t)Qx(t) + \rho u^T(t)Ru(t)] \, dt \tag{4}$$

where Q is a positive semi-definite matrix, R is a positive definite matrix, and ρ is a positive non-zero scalar. The first term penalizes transient deviation of the state from the origin. The second term penalizes the amount of control effort used to control the states. Parameters Q, R, and ρ are weighting terms that adjust the penalties for transient deviation and control effort. The optimization problem is then to find the control $u(t), 0 \leqslant t \leqslant \infty$, that minimizes the performance index J subject to the following dynamic constraints:

(1) the plant is controllable or can be stabilized

(2) the final time is $t = \infty$

(3) $(A, Q^{1/2})$ is observable

The solution for the standard LQR problem is given in [2-4]; therefore, only the results are summarized below. The optimal steady-state solution yields the control law

$$u(t) = -Kx(t) \tag{5}$$

with the feedback gain matrix K defined as

$$K = R^{-1}B^T P \tag{6}$$

where P is a symmetric positive semi-definite solution to the Riccati equation in matrix form

$$A^T P + PA + Q - PBR^{-1}B^T P = 0 \tag{7}$$

Numerical procedures are used to solve the algebraic Riccati equation and calculate K knowing the system and weighting matrices [2]. The LQR optimal design for state feedback control guarantees that the closed-loop system described by Eq. (3) is stable and that the LQR control law (Eq. 5) generates the minimum possible value of the quadratic cost objective J given by Eq. (4). In addition to the nominal closed-loop stability guarantee of analog LQR designs are its properties of robustness. An LQR-based system guarantees an infinite upward gain margin and a gain reduction of at least 1/2, or -6 dB, and a phase margin of at least ±60 degrees. If the final implementation of this controller is in time-discretized (digital) form, then stability is degraded slightly from the continu-

ous case because of finite sampling time. This degradation should be investigated and quantified. A complete discussion of the discrete LQR problem may be found in [2] or [5]. It is stressed that all robustness and performance guarantees for continuous and discrete time LQR designs do not necessarily hold in observer/Kalman-filter-based feedback controllers. This fact may constitute a good argument to use state feedback when the physical states are accessible and do not cost an inordinate amount to sense.

B. The Kalman Filter

Implementation of state feedback requires knowledge of the entire state vector. When states are unmeasured they must be estimated. A closed-loop estimator is based on a plant model and the weighted difference between the estimated and actual output. Figure 1 describes state feedback implementation using an estimator. Typical errors in the estimated state vector may arise from modeling errors and from uncompensated deterministic and stochastic disturbances. These errors are corrected by feedback of the output estimation error with a feedback gain factor. In order to arrive at optimal estimation (or state reconstruction), the choice of this feedback gain can be based on the solution of the classical Kalman filter problem. Such an estimator, or filter, generates unbiased and minimum variance estimates of the plant state variables based upon past sensor measurements and applied controls.

Two of the many good references for optimal estimation theory (both in discrete and continuous time) and its application in optimal control problems are [4] and [5]. The following summarizes the solution to a simplified classical Kalman filter problem. The problem is based on the following stochastic plant dynamics:

$$\dot{x}(t) = Ax(t) + Bu(t) + N\xi(t)$$
$$y(t) = Cx(t) + \theta(t)$$

(8)

where $\xi(t)$ and $\theta(t)$ are assumed to be Gaussian, zero mean, additive white process and sensor noise, with constant intensity matrices Ξ and Θ characterized as follows:

$$\text{covariance } [\xi(t); \xi(\tau)] = E\{\xi(t)\xi^T(\tau)\} = \Xi\delta(t-\tau)$$

$$\Xi = \Xi^T > 0$$

(9)

$$\text{covariance } [\theta(t); \theta(\tau)] = E\{\theta(t)\theta^T(\tau)\} = \Theta\delta(t-\tau)$$

$$\Theta = \Theta^T > 0$$

where $E\{\cdot\}$ is the expectation operator. It is also assumed that $\theta(t)$ is independent of $\xi(t)$. The filter is driven by the control, $u(t)$, and by the noisy measurement vector, $y(t)$, and generates a real-time state estimate and output estimate based on the following filter equations:

$$\dot{\hat{x}}(t) = A\hat{x}(t) + Bu(t) + L[y(t) - C\hat{x}(t)] \; ; \; \hat{x}(0) = E\{x(0)\}$$

$$\hat{y}(t) = C\hat{x}(t)$$

(10)

where L is the optimal feedback gain vector. The choice of L that yields the optimal solution to the formulated estimation problem is

$$L = \Sigma C^T \Theta^{-1}$$

(11)

where the so-called error covariance matrix Σ is calculated from the following filter algebraic Riccati equation (FARE) in matrix form:

$$O = A\Sigma + \Sigma A^T + L\Xi L^T - \Sigma C^T \Theta^{-1} C\Sigma$$

(12)

A unique, steady-state, positive semi-definite solution matrix Σ to Eq. (12) exists if the following conditions are met:

(1) [A,N] is stabilizable

(2) [A,C] is detectable

Numerical solution methods to the FARE are given in [4]. The estimation error dynamics are obtained by subtracting Eq. (10) from Eq. (8) to yield

$$\dot{\tilde{x}}(t) = (A - LC)\tilde{x}(t) + L\xi(t)$$

(13)

Thus, the error dynamics can be shown to be dependent on the selection of L. The optimality of the Kalman filter can be interpreted as follows: if the measurements started at $t = -\infty$, then the state estimation vector has zero mean, i.e.,

$$E\{\tilde{x}(t)\} = E\{x(t) - \hat{x}(t)\} = 0$$

(14)

and the optimal error covariance matrix is Σ, i.e.,

$$\Sigma = E\{\tilde{x}(t)\tilde{x}^T(t)\}$$

(15)

such that any other gain L will yield state estimation errors with *larger* variances. Given the stabilizability and detectability assumptions of the stochastic plant dynamics, the Kalman filter, viewed as a dynamic feedback system described by the state equations of Eq. (10), is guaranteed to be stable. Thus the eigenvalues of $(A - LC)$ are strictly in the left-half s-plane.

III. Modeling

The LQG tracking controller designs for the 70-m axis servos are based on simplified fourth-order rate loop models. Figure 2 presents the linear model for the rate loops of the 70-m Az-El antenna. Shown is the computer mode of operation. Since the physical hardware designs for the Az and El axis rate loops differ very slightly, only the Az rate loop model and controller design are presented. A high-order theoretical model was simplified by eliminating fast dynamics and normalizing to yield the transfer function:

$$G(s) = \frac{Y(s)}{U(s)}$$

$$= \frac{83.5\,(s + 80)\,(s + 4.4)}{(s + 61.25)\,(s + 2.39)\,[(s + 8.75)^2 + (11.36)^2]}$$

(16)

where $U(s)$ is the input rate in degrees per second and $Y(s)$ is output rate in degrees per second. The simplified model in Eq. (16) represents a rigid antenna model.

Verification of the simple rate loop model of Eq. (16) was accomplished by using an HP 3562A dynamic signal analyzer

to measure the swept sinusoidal frequency response of the azimuth rate loop at DSS-14. Figures 3 and 4 present the measured gain and phase responses, respectively. These responses were compared with the simplified theoretical model. The accuracy of the approximation is illustrated by superimposing measured data upon the frequency response of the theoretical transfer function (Eq. 16), shown in Figs. 5 and 6.

The design of the LQR and Kalman filter require a state-space representation of the plant model. The plant transfer function, Eq. (16), was transferred into a diagonal canonical set of state-space equations of the form of Eq. (1) to yield

$$\dot{x}(t) =$$

$$\begin{bmatrix} -61.25 & 0 & 0 & 0 \\ 0 & -8.747 & 11.360 & 0 \\ 0 & -11.360 & -8.747 & 0 \\ 0 & 0 & 0 & -2.393 \end{bmatrix} x(t) + \begin{bmatrix} 0.7239 \\ -0.1982 \\ 0.9802 \\ 1.1421 \end{bmatrix} u(t)$$

$$y(t) =$$

$$[\,0.7239 \quad 9.226 \quad 0 \quad 1.1421\,]\,x(t)$$

(17)

where u is input rate and y is output rate. The state equations were then augmented to include states for position and integral of position. The augmented matrices are formed by using the output vector C to form the integration of rate or position state and then adding the integration of position to form an integral of position state. The result for azimuth is

$$\dot{x}(t) = \begin{bmatrix} 0 & 1 & 0 & 0 & 0 & 0 \\ 0 & 0 & 0.7239 & 9.226 & 0 & 1.1421 \\ 0 & 0 & -61.25 & 0 & 0 & 0 \\ 0 & 0 & 0 & -8.747 & 11.360 & 0 \\ 0 & 0 & 0 & -11.360 & -8.747 & 0 \\ 0 & 0 & 0 & 0 & 0 & -2.393 \end{bmatrix} x(t) + \begin{bmatrix} 0 \\ 0 \\ 0.7239 \\ -0.1982 \\ 0.9802 \\ 1.1421 \end{bmatrix} u(t)$$

$$y(t) = [\,0 \quad 1 \quad 0 \quad 0 \quad 0 \quad 0\,]\,x(t)$$

(18)

Augmenting increased the dimension of **A** from 4 X 4 to 6 X 6, the dimension of **B** from 4 X 1 to 6 X 1, and the dimension of **C** from 1 X 4 to 1 X 6. The diagonal canonical form of the state equations was used to reduce computation and to ensure reasonable matrix numerical conditioning. Equation (18) describes a regulator, and will be used in the LQR design process.

IV. Linear Quadratic Regulator Design

The ultimate goal is to design an optimal tracking controller for the 70-m Az axis servo. However, the solution to a linear quadratic deterministic reference input tracking problem requires knowledge of the future values of the command input. For tracking systems in which the reference input is generated by an exogenous source, this uncertainty must be suitably translated to a stochastic optimization problem [4]. A different approach, taken in this article, was to proceed with an LQR design for the dynamic system of Eq. (18) and then adapt it to track command inputs. A visualization of this so-called LQ servo is presented in Fig. 7, in which the position state becomes the position error and the integral of position becomes the integral of position error. It is noted that the properties of the resultant LQR do not directly reflect the command-following properties of the LQ servo, which will ultimately dictate the choice of the final controller.

The LQR design depends on the selection of weighting matrices, which requires intuition and iteration. For the 70-m servo controller, the **Q** matrix is 6 X 6, ρ is scalar, and **R** is taken to be the identity matrix. A general approach was used for the choice of the weighting matrix coefficients. The **Q** matrix is a unit diagonal with two modifications. First, eigenvalues of the **A** matrix which have a value greater than the foldover frequency are given minimal weighting. The final implementation of the controller is time-discretized with a sampling frequency of f = 20 Hz, so the foldover frequency computed by the formula $(f/2)$ 2 PI is 62.8 radians/second. The eigenvalue at -60.80 is close to the foldover frequency and is therefore weighted lightly to minimize control effort applied to the eigenvalue frequency. The weighting matrix **Q** takes the form

$$Q = \begin{bmatrix} 1 & 0 & 0 & 0 & 0 & 0 \\ 0 & 1 & 0 & 0 & 0 & 0 \\ 0 & 0 & 0.0001 & 0 & 0 & 0 \\ 0 & 0 & 0 & 1 & 0 & 0 \\ 0 & 0 & 0 & 0 & 1 & 0 \\ 0 & 0 & 0 & 0 & 0 & 1 \end{bmatrix} \quad (19)$$

The second modification to the unit diagonal structure of **Q** allows the designer flexibility in selecting the optimal dynamics. The element Q_{11} is varied to provide greater weight on the integral error state and thus minimize tracking error. In addition to iterating Q_{11} to achieve desirable closed-loop performance and robustness, the scalar ρ is varied. In general, increasing the value of ρ increases penalty on the control and results in lower bandwidth designs, while conversely, a lower value of ρ produces higher bandwidths because penalty on control effort is decreased. Figure 8 presents various closed-position loop step responses corresponding to various LQ-based designs obtained by setting Q_{11} equal to 4 and iterating ρ. As the simulations indicate, the higher values of ρ result in closed-loop responses exhibiting slightly larger overshoots and longer settling times.

The final LQ-servo controller design chosen must achieve a desired bandwidth, step response overshoot, and settling time, and ensure satisfactory robustness properties. Robustness evaluation must take into account parameter changes in the rate loop model that do not directly correspond to changes in the forward gain of the position loop, which defines the classical characteristics of gain and phase margin. The final iteration results (based on the continuous time model) are presented below:

Q_{11}	ρ	k_1	k_2	k_3	k_4	k_5	k_6
4	10	0.6325	1.3417	0.0157	0.5338	0.6613	0.5270

Closed-loop poles, rad/sec: -0.564 ±0.541j, -2.4159, -8.7496 ±11.3605j, -61.25

Settling time: 5.7 sec

Percent overshoot: 25.2 percent

Figures 9, 10, and 11 show the open-loop and closed-loop frequency responses and the step response using the gain vector chosen above. The gain margin for this continuous time design is infinite and the phase margin is 65 deg. The tracking bandwidth is approximately 0.259 Hz. These values of the resultant LQ-servo design indicate that this optimal feedback vector yields a robust controller design.

V. The Kalman Filter Design

The Kalman filter design procedure consisted of selecting estimator dynamics and computing the filter gain vector. The integral-of-position error is easily obtained in real time by numerical integration, therefore a fifth-order Kalman filter was designed using the continuous plant model of Eq. (1) (excluding the first equation). Presently, the encoder feedback to the

estimator is assumed to be a smooth DC signal and no convenient mathematical model is available to characterize any associated noise. Thus the measurement noise intensity Θ can be utilized as a parameter in the filter design. Obviously, the different optimal gain vectors L will result for each choice of the filter parameters Θ and the process noise intensity matrix Ξ, which are both defined by Eq. (9). In this design the Loop Transfer Recovery (LTR) method is used to conveniently characterize these noise statistics of the stochastic plant model (Eq. 8).

A formal discussion of the LTR method is given in [6, 7], where it is applied to multivariable-error-only control systems in conjunction with LQR designs to form so-called LQG/LTR feedforward compensators. Here, in the iteration process of calculating and evaluating the optimal filter gains, the results of the LTR method are used to effectively reduce the parameterization to one scalar variable μ. The method defines the noise intensities to be

$$\Xi \triangleq BB^T$$
$$\Theta \triangleq \mu I \tag{20}$$

The design parameter is varied and the PC-based control system package PROGRAM CC is used to solve the resulting filter algebraic Riccati equation and compute L. The Kalman filter performance is based on position response, estimator error dynamics, and noise rejection ability. The LQR and filter design are combined to form the LQG controller, and its position response should display the same performance as discussed for the LQ servo. The error dynamics should have adequate speed of response and minimal overshoot. The noise rejection of the LQG controllers is evaluated through simulations which include nonlinear plant dynamics, antenna structural dynamics, and encoder and D/A quantization effects. Several iterations of μ were made and the final Kalman filter design was chosen to be the following

μ	L_1	L_2	L_3	L_4	L_5	L_6
5	0.00	0.4118	0.00005	0.00311	-0.00048	0.04912

Closed-loop filter poles, rad/sec:	-0.4045, -2.5146,
	-8.9027 $\pm$11.4776j,
	-61.2521

VI. Simulation Results

The final implementation of the LQG controller is a time-discretized form. The linear system matrices A and B of Eq. (18) are transformed from the continuous time domain to the discrete (sampled data) time domain via sampling described by

a zero-order hold to produce the necessary discrete time system matrices. The computations of the discrete system matrices are based on a specific (50-msec) sample interval and negligible time delay between each encoder input and the corresponding rate command output. Both LQ and Kalman filter gains designed for the continuous plant model (Eq. 18) are used with the discrete system matrices in the controller algorithm. Through simulations, the difference between the system response of the LQG controller with both the continuous and discrete state-space matrices has been shown to be negligible. Readers are referred to [8] for a more in-depth review of the implementation of the digital computer-based controller.

Simulations for the continuous linear antenna model with the final discretized LQG controller are presented in Figs. 12-15. Shown are the position, position estimation error, and rate input command responses for a 10-mdeg-step input with zero initial conditions. The position response exhibits the same performance as that of the LQ-servo response of Fig. 11 except for a slight lag due to the digitized controller. The estimation error response of Fig. 13 is due to the discretization of the controller and exhibits a desired speed of response and minimal error overshoot. The commanded rate of Fig. 14 is an ideal smooth, decreasing function.

A more accurate performance evaluation is based on the nonlinear simulation models developed in [9]. The results for a 10-mdeg-step input are shown in Figs. 15-17, where now the position is the output of a 20-bit encoder, the estimation error is the difference between encoder output and estimated position, and the commanded rate is equivalent to the output of the D/A converter. The position response of Fig. 15 illustrates the encoder quantizing effects and additional small time lags (at time zero and at 2.8 sec) due to the friction associated with the hydraulic motor and gear reducer. However, performance characteristics are not severely degraded from those shown for the linear system of Fig. 12. The position estimation error response of Fig. 16 shows roughly the same dynamics of the initial error transient as the linear case of Fig. 13. The peak estimation error is 0.6 mdeg, which corresponds to approximately two least-significant encoder bits (0.0003433 deg/bit) for the 20-bit encoders. Each new position quantization level causes a step in estimation error with peak magnitude of one encoder bit as shown. The rate command of Fig. 17 is seen to be a decreasing function that oscillates between D/A quantization levels. The overall performance of this selected LQG controller is deemed satisfactory.

VII. Summary

The Linear Quadratic Gaussian (LQG) optimal control method has been presented and applied to develop a new type-II, state-feedback antenna position controller. Theory on

the controller and state estimation techniques (specifically the Linear Quadratic Regulator and Kalman filter), which when combined make up the LQG design, was presented. A simplified experimental transfer function model was developed and mapped into a diagonal canonical set of state equations. The model was then augmented to include position and integral-of-position to form the final design plant model. Next an LQR was designed for this system and adapted for command following; the result is the so-called LQ servo. Finally, a new method for choosing the Kalman filter gains using the Loop Transfer Recovery method was presented. Performance specifications dictated the selection of the final gain vectors. Linear and non-linear simulation results were presented.

VIII. Potential Improvements

The final LQG controller gain selections were based on performance specifications. However, design methods for the dynamic plant estimator can be improved further. Investigations are needed which will determine the estimator design criteria which take into account encoder quantization effects. Given this, the systematic LQG design process can be reapplied. Also, LQG/LTR error-only controllers as discussed in [6] should be developed for the precision mode of operation and be simulated against the current LQG controllers to evaluate any performance gains. The motivation for such an effort is that the Kalman filter (which estimates antenna rate and higher derivatives in precision mode) will now be driven by autocollimator measurements instead of encoder readings. Thus, quantization errors associated with the axis encoders can be avoided and high-resolution estimates based on the auto-collimator signals will result. Both future position controller and estimator design work would utilize currently known values of the system nonlinearities, structure dynamics test data, estimates of modeling errors, and system component/disturbance stochastic models.

References

[1] J. A. Nickerson, "A New Linear Quadratic Optimal Controller for the 34-Meter High Efficiency Antenna Position Loop," *TDA Progress Report 42-90*, vol. April–June 1987, Jet Propulsion Laboratory, Pasadena, California, pp. 136–147, August 15, 1987.

[2] G. F. Franklin and J. D. Powell, *Digital Control of Dynamic Systems*, Reading, Massachusetts: Addison-Wesley Publishing Co., 1980.

[3] A. E. Bryson, Jr. and Y. Ho, *Applied Optimal Control*, Waltham, Massachusetts: Balisdell Publishing Co., 1969.

[4] H. Kwakernaak and R. Sivan, *Linear Optimal Control Systems*, New York: John Wiley and Sons, Inc., 1972.

[5] K. J. Astrom and B. Wittenmark, *Computer Controlled Systems: Theory and Design*, Reading, Massachusetts: Addison-Wesley Publishing Co., 1980.

[6] G. Stein and M. Athans, "The LQG/LTR Procedure for Multivariable Control Design," *IEEE Trans. Automatic Control*, vol. AC-32, no. 2, pp. 105–114, February 1987.

[7] J. C. Doyle and G. Stein, "Multivariable Feedback Design: Concepts for a Classical/ Modern Synthesis." *IEEE Trans. Automatic Control*, vol. AC-26, pp. 4–16, February 1981.

[8] R. E. Hill, "A Modern Control Theory Based Algorithm for Control of the NASA/ JPL 70-Meter Antenna Axis Servos," *TDA Progress Report 42-91*, vol. July–September. Jet Propulsion Laboratory, Pasadena, California, pp. 285–294, November 15, 1987.
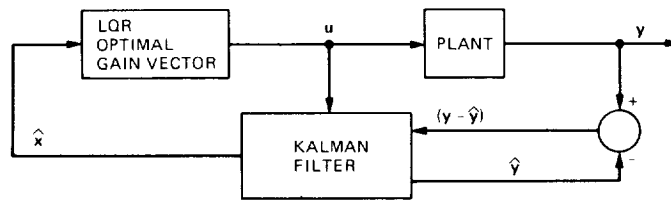
[9] R. E. Hill, "Dynamic Models for Simulation of the 70-M Antenna Axis Servos," *TDA Progress Report 42-95*, vol. July–September 1988, Jet Propulsion Laboratory, Pasadena, California, pp. 32–50, November 15, 1988.

Fig. 1. State feedback with a Kalman estimator for a continuous time regulator.
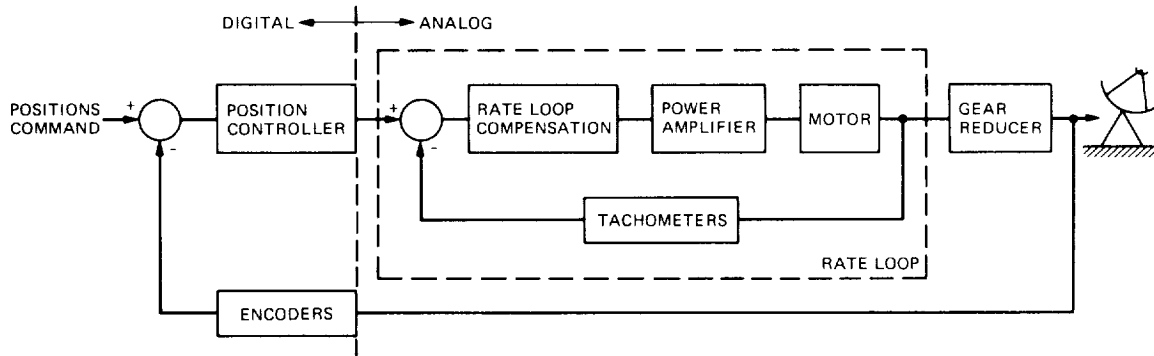
Fig. 2. Rate loop model.
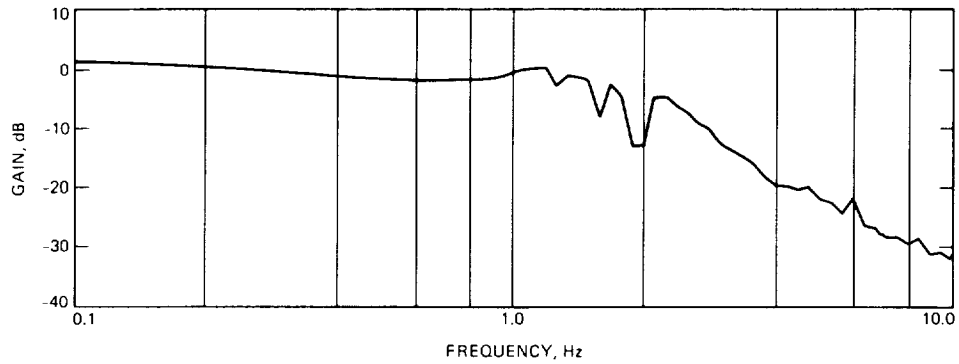
Fig. 3. DSS-14 azimuth rate loop gain response.
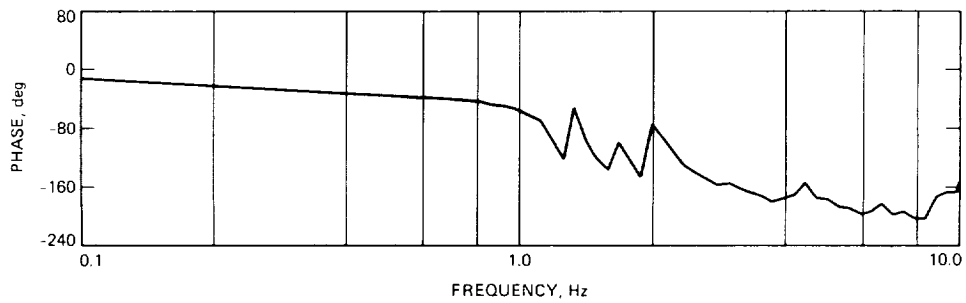
Fig. 4. DSS-14 azimuth rate loop phase response.
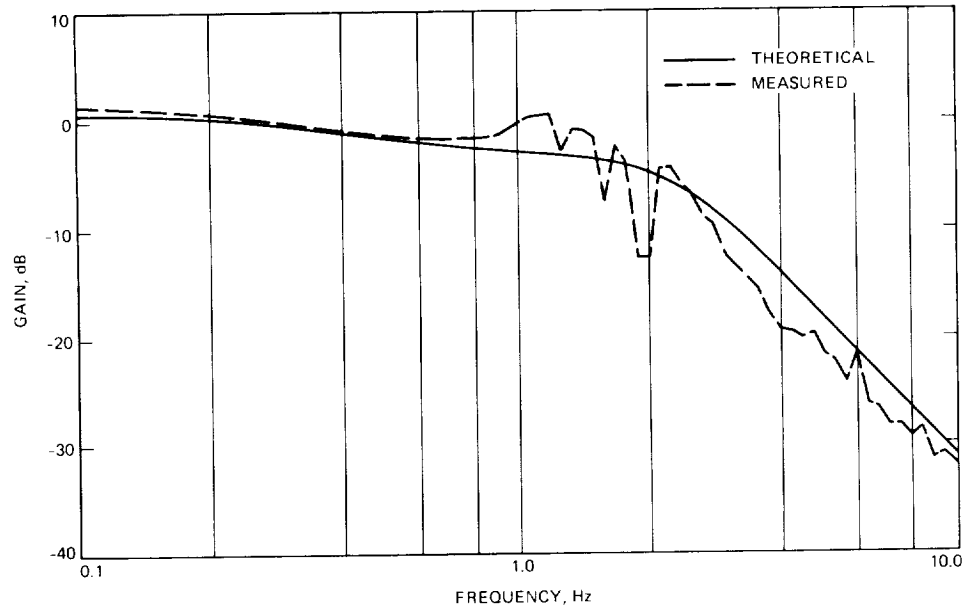
Fig. 5. Comparison of measured and theoretical gain response.
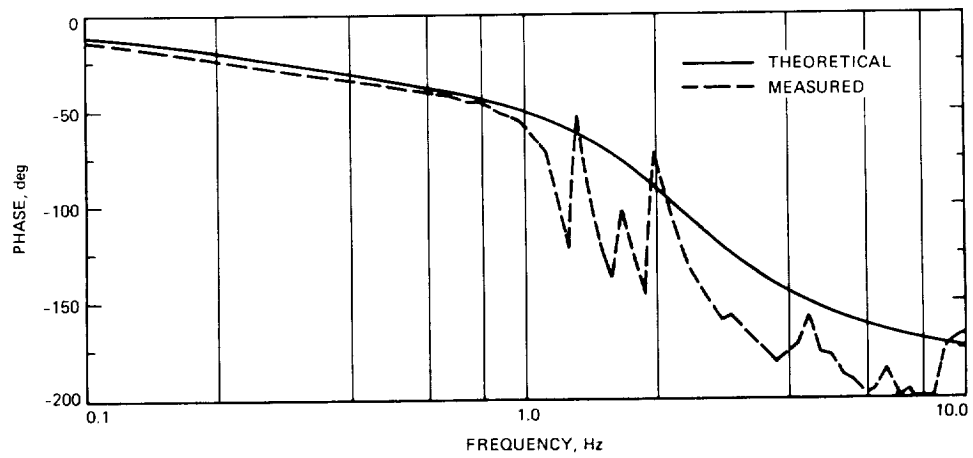
Fig. 6. Comparison of measured and theoretical phase response.
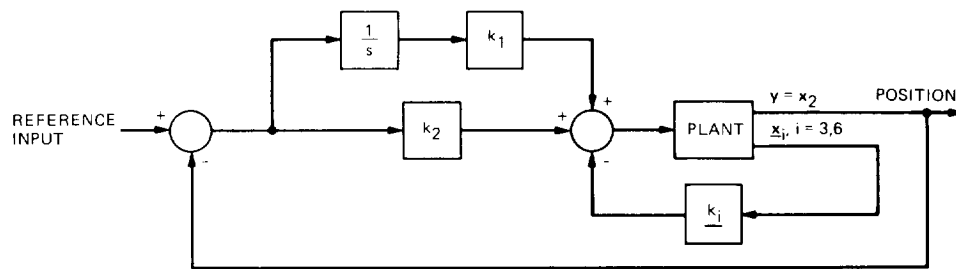
Fig. 7. Visualization of LQ servo.
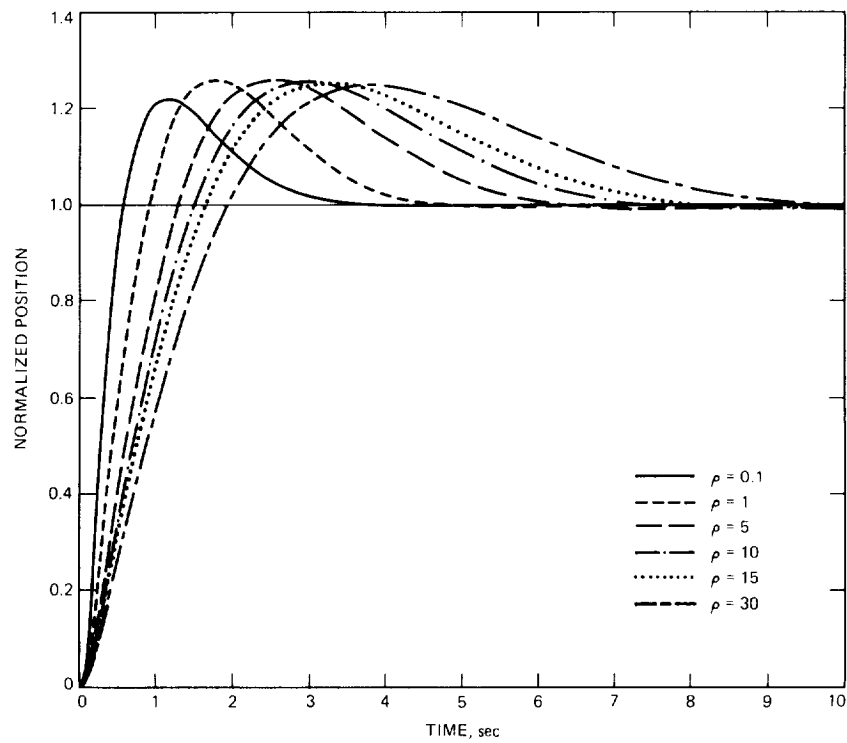
Fig. 8. Normalized step responses for $Q_{11} = 4$.
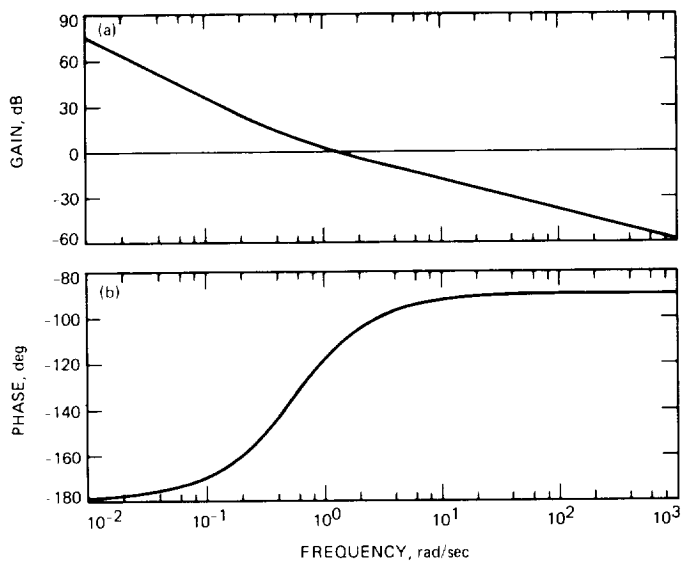
Fig. 9. Open-loop frequency responses for final LQ-servo design: (a) gain, and (b) phase.
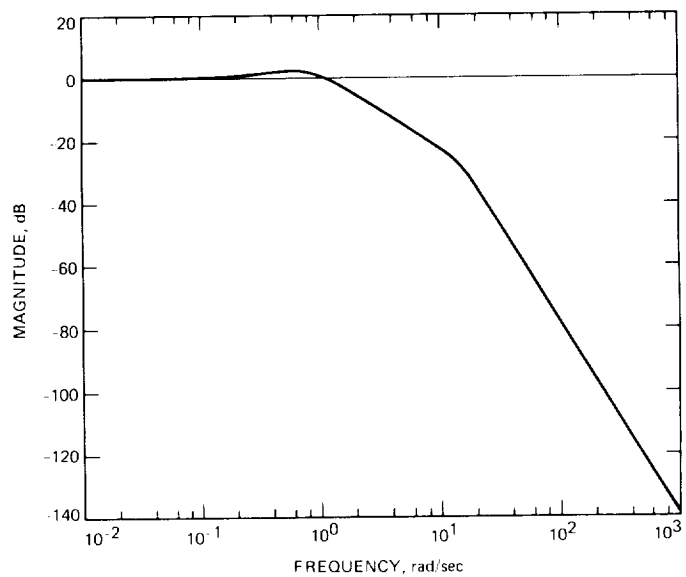
Fig. 10. Closed-loop Bode magnitude plot for final LQ-servo design.
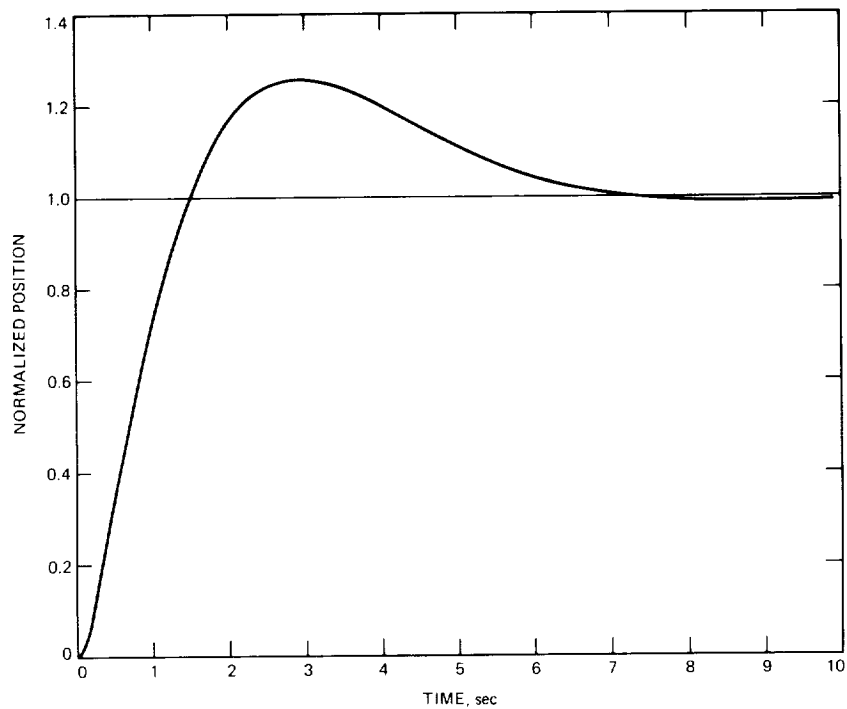
Fig. 11. LQ-servo step response.
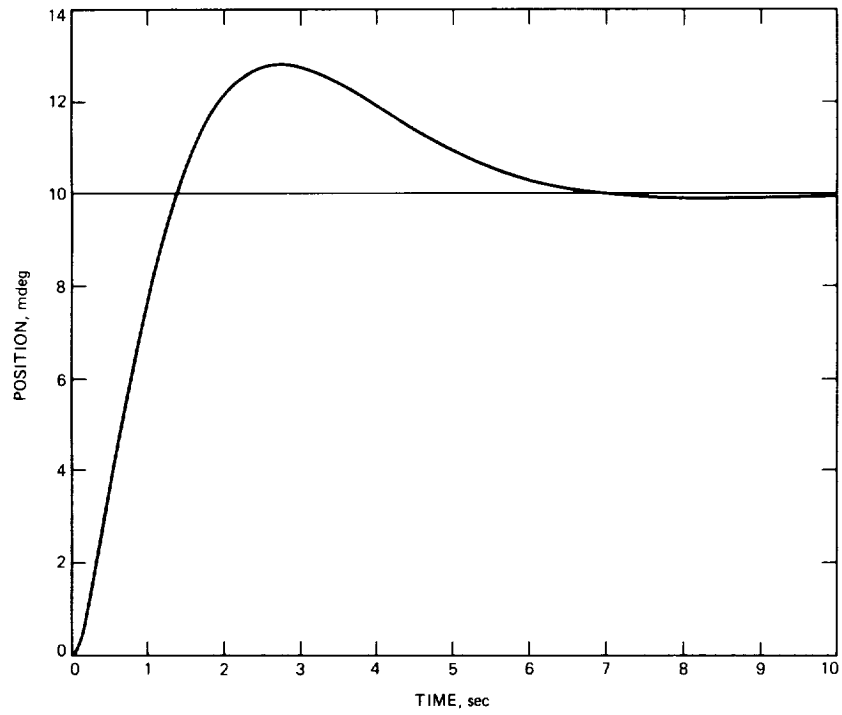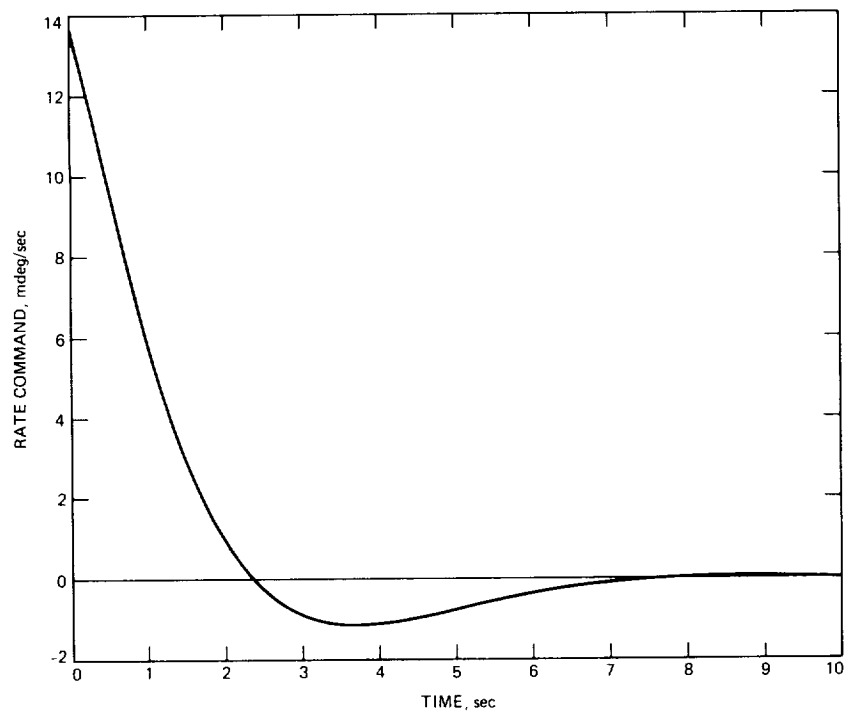
Fig. 12. LQG step response.
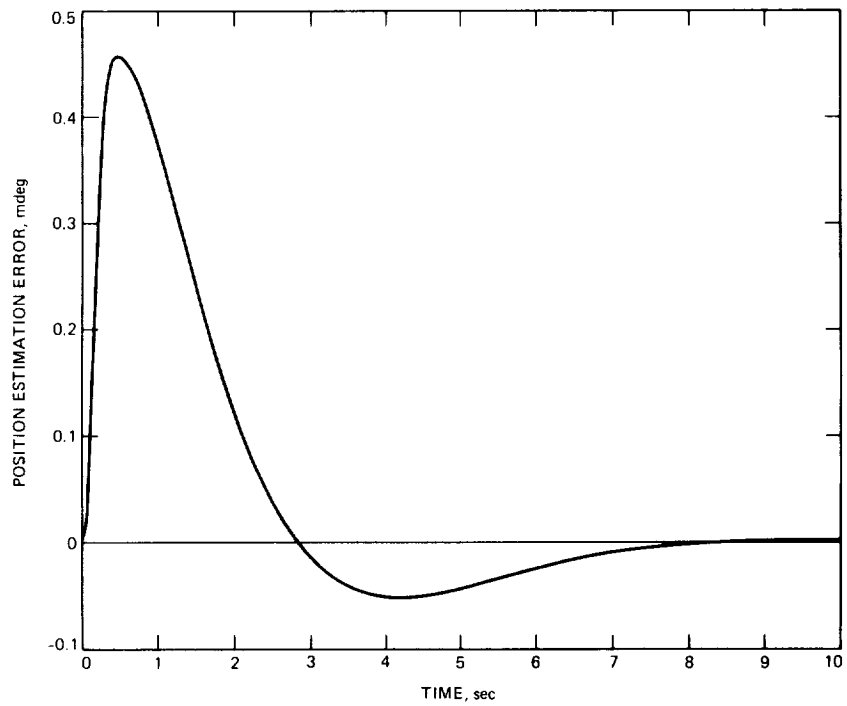
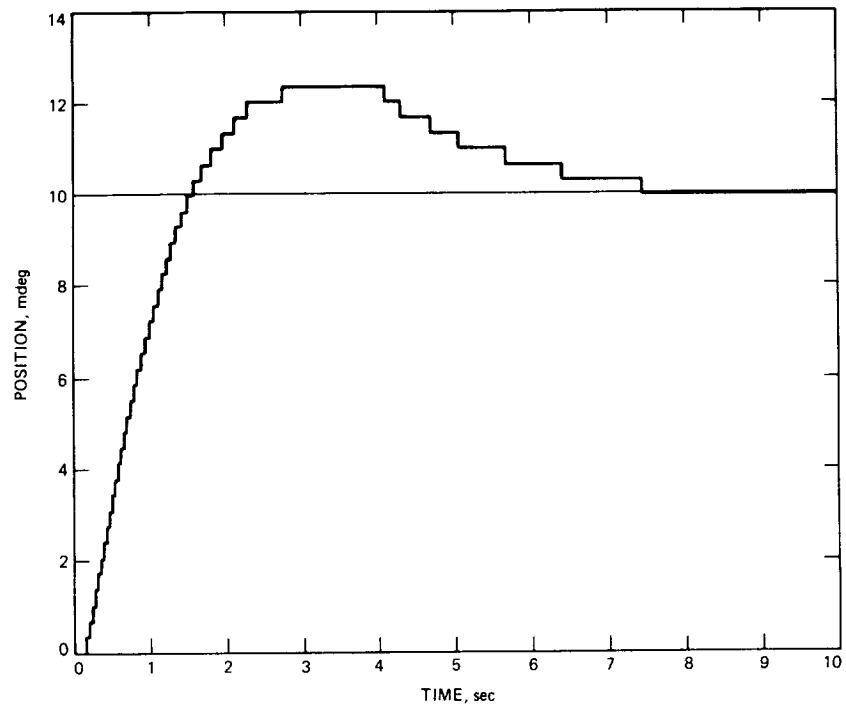Fig. 13. LQG position estimation error.

Fig. 14. LQG rate command.
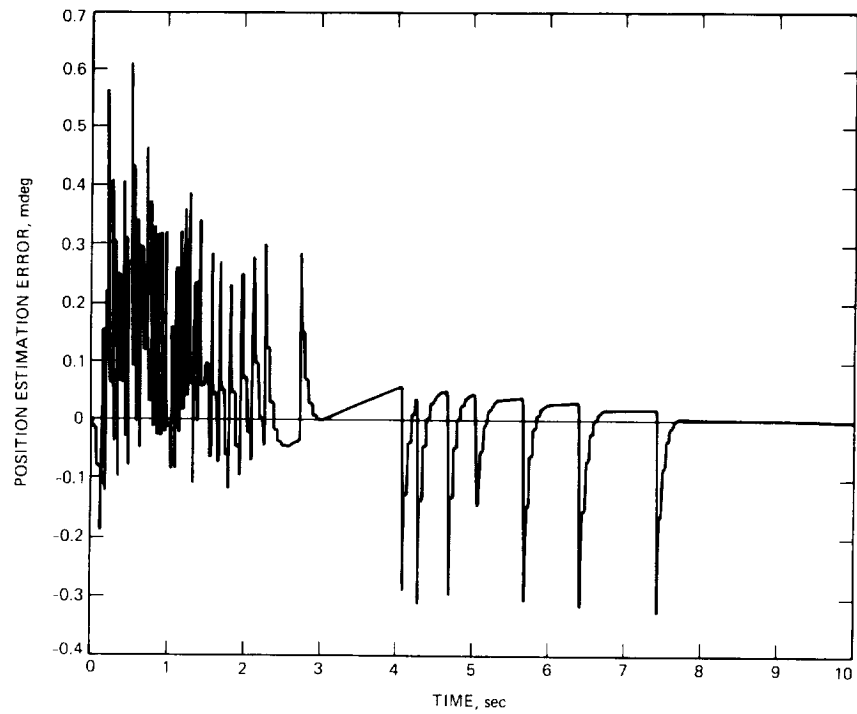

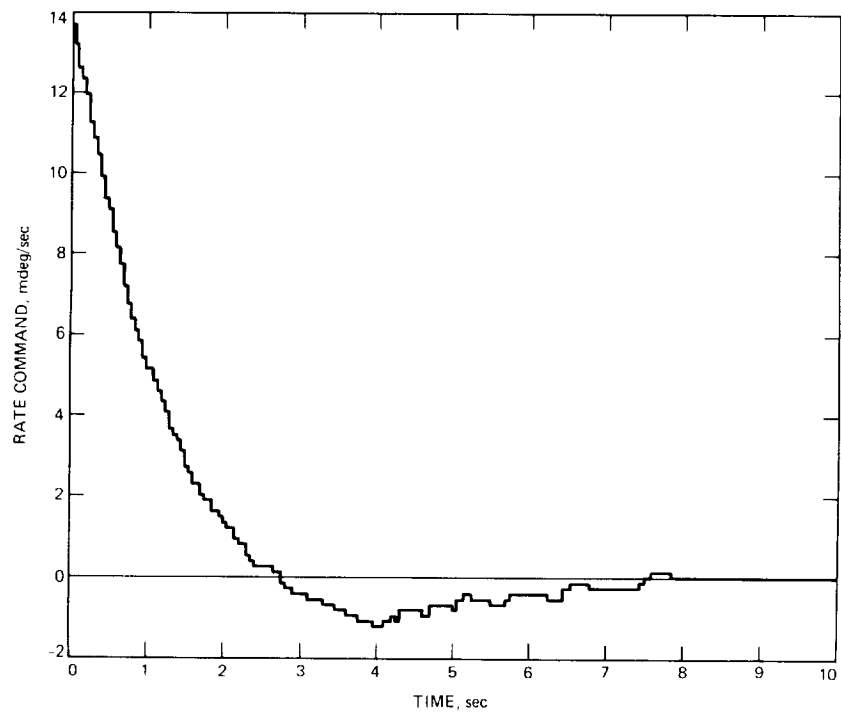**Fig. 15. Nonlinear position response.**

Fig. 16. Nonlinear position estimation error.

Fig. 17. Nonlinear rate command.